

Characterizing Natural Hydrogen Occurrences in the Paris Basin Using OCR-Enhanced Well Database Studies

Nicolas Lefeuvre¹, Eric Thomas², Laurent Truche³, Frédéric-Victor Donzé⁴, Thibault Cros², Johann Dupuy², Laura Alejandra Pinzon-Rincon⁵, and Christophe Rigollet²

¹Université Grenoble Alpes

²CVA Group

³ISTerre, UMR 5275 of CNRS, University of Grenoble Alpes, F-38041 Grenoble Cedex 9, France.

⁴Institut des Sciences de la Terre

⁵Univ. Grenoble Alpes

January 23, 2024

Abstract

This study investigates natural hydrogen (H₂) occurrences in the Paris Basin, using Optical Character Recognition (OCR) technology to analyze an extensive, yet historically underexploited, well database that contains older drilling records. With the growing demand for carbon-free energy, natural hydrogen, produced through processes like serpentinization and water radiolysis, offers a promising alternative to fossil fuels. However, its potential has been largely unexplored in conventional oil and gas wells. Utilizing the BEPH (Office of Exploration and Production of Hydrocarbons) French database, which includes well logs, mudlogs, and End Drilling Reports (EDRs) in PDF image format, we applied the Tesseract-OCR Engine to convert these documents into searchable formats for efficient data analysis. Our analysis revealed several H₂-bearing wells across the French sedimentary basins. The hydrogen occurrences in the Aquitaine Basin correlate with the geological context, but those in the Paris Basin present an anomaly, as their H₂ occurrences do not align with the expected geological factors. In the Paris Basin, H₂ has been detected in four main formations: the Lusitanian aquifer, Dogger aquifer, Triassic aquifer, and the basement. The highest hydrogen concentration (52 vol%) was found in the Dogger formation. These wells are primarily located along the Bray fault and thrust, indicating a geological influence on H₂ distribution. This research demonstrates the effectiveness of OCR in reprocessing historical drilling data for natural hydrogen exploration, highlighting the need for comprehensive exploration methodologies in this emerging field.

Hosted file

985034_0_art_file_11788292_s7qxqj.docx available at <https://authorea.com/users/527801/articles/705574-characterizing-natural-hydrogen-occurrences-in-the-paris-basin-using-ocr-enhanced-well-database-studies>

Hosted file

985034_0_supp_11788468_s77y48.docx available at <https://authorea.com/users/527801/articles/705574-characterizing-natural-hydrogen-occurrences-in-the-paris-basin-using-ocr-enhanced-well-database-studies>

1
2
3
4
5
6
7
8
9
10
11
12
13

Characterizing Natural Hydrogen Occurrences in the Paris Basin Using OCR-Enhanced Well Database Studies

Nicolas Lefeuvre^{1,2,*}, Eric Thomas², Laurent Truche¹, Frédéric-Victor Donzé¹, Thibault Cros², Johann Dupuy², Laura Pinzon-Rincon¹, Christophe Rigollet²

¹ Université Grenoble Alpes, CNRS, ISTerre, F-38058 Grenoble Cedex 9, France.

² CVA Group, 2 rue Myron Kinley, 64000 Pau – France

Corresponding author: Nicolas Lefeuvre (nicolas.lefeuvre@univ-grenoble-alpes.fr)

Key Points:

- Natural hydrogen exploration in former oil & gas province.
- Use of OCR algorithm to optimize processing of a large drilling report database.
- Indices of a potential new H₂ system (source, migration, trap) in the Paris Basin.

14 **Abstract**

15 This study investigates natural hydrogen (H₂) occurrences in the Paris Basin, using Optical
16 Character Recognition (OCR) technology to analyze an extensive, yet historically
17 underexploited, well database that contains older drilling records. With the growing demand for
18 carbon-free energy, natural hydrogen, produced through processes like serpentinization and
19 water radiolysis, offers a promising alternative to fossil fuels. However, its potential has been
20 largely unexplored in conventional oil and gas wells. Utilizing the BEPH (Office of Exploration
21 and Production of Hydrocarbons) French database, which includes well logs, mudlogs, and End
22 Drilling Reports (EDRs) in PDF image format, we applied the Tesseract-OCR Engine to convert
23 these documents into searchable formats for efficient data analysis. Our analysis revealed several
24 H₂-bearing wells across the French sedimentary basins. The hydrogen occurrences in the
25 Aquitaine Basin correlate with the geological context, but those in the Paris Basin present an
26 anomaly, as their H₂ occurrences do not align with the expected geological factors. In the Paris
27 Basin, H₂ has been detected in four main formations: the Lusitanian aquifer, Dogger aquifer,
28 Triassic aquifer, and the basement. The highest hydrogen concentration (52 vol%) was found in
29 the Dogger formation. These wells are primarily located along the Bray fault and thrust,
30 indicating a geological influence on H₂ distribution. This research demonstrates the effectiveness
31 of OCR in reprocessing historical drilling data for natural hydrogen exploration, highlighting the
32 need for comprehensive exploration methodologies in this emerging field.

33 **Plain Language Summary**

34 This study explores the presence of natural hydrogen (H₂) in the Paris Basin, employing Optical
35 Character Recognition (OCR) technology to sift through an extensive database of older drilling
36 records that have not been fully utilized in the past. As the world increasingly seeks carbon-
37 neutral energy sources, natural hydrogen, produced through interactions between water and
38 rocks, emerges as a promising alternative to fossil fuels.

39 Our research focuses on the BEPH (Office of Exploration and Production of Hydrocarbons)
40 French database, which contains detailed information on drilling activities, but in a non-
41 searchable PDF image format. OCR is a tool that turns images containing text, like scanned
42 documents, into text files that we can easily search and analyze.

43 Our findings indicate the presence of H₂ in several wells across the French sedimentary basins.
44 Particularly intriguing are the results from the Aquitaine Basin, where hydrogen occurrences
45 align with the geological context, and the Paris Basin, which exhibits unexpected H₂ occurrences
46 not directly linked to anticipated geological factors known for H₂ exploration. In the Paris Basin,
47 the highest hydrogen concentration (52 vol%) was discovered in the Dogger formation. These
48 wells are predominantly situated along the Bray fault and thrust, suggesting a geological
49 influence on the distribution of hydrogen.

50 This research underscores the utility of OCR technology in re-evaluating historical drilling data
51 for natural hydrogen exploration. It highlights the necessity for thorough exploration strategies in
52 this nascent yet promising field.

53 **1 Introduction**

54 Geochemical interactions between water and rock on Earth are known to generate molecular hydrogen
55 (H₂). This process, extensively documented in the literature (e.g., Klein et al., 2020), includes the
56 serpentinization of ultramafic rocks which is a reaction characterized by the hydration of olivine and
57 pyroxene minerals to form serpentine, brucite, and magnetite, accompanied by H₂ production (Malvoisin
58 et al., 2012; Marcaillou et al., 2011; Mayhew et al., 2013; McCollom and Donaldson, 2016). Additionally,
59 water radiolysis, which involves the dissociation of water molecules into H₂ and O₂ due to radiation, also
60 contributes to H₂ generation (Lin et al., 2005; Sauvage et al., 2021; Warr et al., 2019). These geochemical
61 processes are not only crucial for understanding Earth's deep microbial ecosystems but also play a
62 significant role in the abiotic synthesis of organic molecules, as evidenced by numerous studies (Etiopie et
63 al., 2015; Fiebig et al., 2007; Johnson et al., 2015; Lin et al., 2005; Sherwood Lollar et al., 2006).

64 In light of the global shift towards sustainable energy sources, naturally occurring H₂ has garnered
65 significant attention as a viable, carbon-neutral energy alternative to traditional fossil fuels. This interest
66 is reflected in recent research exploring the potential of H₂ in various geological contexts (Donzé et al.,
67 2020; Moretti et al., 2021; Prinzhofner et al., 2018; Smith et al., 2005; Truche et al., 2018). Current
68 exploration methodologies for targeting H₂ in potential geological reservoirs predominantly rely on soil
69 gas analysis at a depth of approximately 1 meter. However, this approach is somewhat limited in scope
70 and does not encompass a comprehensive and efficient methodology. This gap in methodology
71 underscores the need for more integrated and systematic exploration strategies, as highlighted in recent
72 studies (Lefeuvre et al., 2022, 2021).

73 In the domain of petroleum geology, the presence of molecular hydrogen in natural reservoirs has
74 historically been underappreciated. This oversight can be attributed to the fact that H₂ was rarely detected
75 in the multitude of wells drilled globally for oil and natural gas exploration, as noted by Gaucher (2020).
76 The standard geochemical sensors employed in these wells were primarily calibrated for detecting fossil
77 hydrocarbons, such as methane, with less sensitivity or focus on H₂.

78 However, emerging research and field data have begun to challenge this long-standing viewpoint. Recent
79 studies have identified significant concentrations of H₂ in various geological settings across the world.
80 Notable examples include the “Bougou-1” well, which was drilled in 1987 in Mali, the concentration of
81 H₂ was found to be 98 vol% (Maiga et al., 2023). The “Tisovita well”, which was drilled before 1978 in
82 Romania, the concentration of H₂ was found to be 28.7 vol% (Mitrofan et al., 2021). The “#1 Wilson
83 Well” drilled in 2006 in the Kansas (USA). the H₂ concentration measured was 10.0 vol% (Newcombe,
84 1935). The well EVDD008 drilled in the Yilgarn Craton, in Australia, the H₂ concentration measured was
85 42.7 mol% (Boreham et al., 2021). At the “Copper Cliff well”, in Canada, the H₂ concentration ranged
86 from 9.9 to 57.8 vol% (Sherwood et al., 1988)

87 These findings underscore the potential for natural hydrogen reservoirs and highlight the necessity for
88 refined geochemical analysis techniques in hydrocarbon exploration, particularly for the detection and
89 quantification of H₂. The implications of these discoveries are significant, not only for understanding
90 subsurface geochemical processes but also for evaluating the potential of H₂ as an energy resource in the
91 context of a transitioning global energy landscape.

92 In France, the exploration and production of oil and gas have led to the drilling of over 5,000 wells.
93 However, none of these wells have been designed for natural hydrogen exploration. The BEPH (Office of
94 Exploration and Production of Hydrocarbons) database used in this study is composed of well logs,
95 mudlogs and End Drilling Reports (EDRs) which are in PDF image format. Manual examination of each
96 well would take a considerable amount of time, so an Optical Character Recognition (OCR) algorithm
97 (Tesseract-OCR google Engine; Smith, 2007) was used to transform these scanned image PDFs into
98 searchable PDFs.

99 Through the analysis of an extensive dataset, we have identified several H₂-bearing wells distributed
100 across the French sedimentary basin (Fig. 1). These wells can be categorized into two distinct groups:
101 those situated in the eastern region of Paris, and those in the southern part of the Aquitaine Basin.

102



103 Figure 1 : Geological map of France highlighting the locations of wells where H₂ occurrences were
 104 detected using OCR.

105

106 In the Aquitain Basin, the observed concentrations of H₂ can be linked to the geological context. Indeed,
 107 these wells are at the vicinity of a mantle body (peridotite) present at relatively shallow depths and are
 108 also near major drain facilitating fluid migration (Chevrot et al., 2022, 2018; Jammes et al., 2010;
 109 Lehujeur et al., 2021; Tugend et al., 2014).

110 In the Paris Basin the H₂-bearing wells are an enigma, as the H₂ occurrences cannot be readily explained
 111 by the local geology. Consequently, our study will focus on investigating the underlying geological
 112 factors influencing H₂ presence in the Paris Basin. Our findings reveal promising indications of H₂
 113 potential in the Paris Basin. This intracratonic basin is characterized by a geologically diverse basement,
 114 comprising peridotite rocks at relatively shallow depths (less than 4 kilometers; Averbuch and Piromallo,

115 2012). Notably, the basin is intersected by major faults that extend through both the basement and the
116 overlying sedimentary cover, which could be conduits for H₂ migration and accumulation.
117 The primary objective of this study is to demonstrate the efficacy of applying OCR technology to old but
118 extensive drilling datasets. This approach enables the rapid identification of unexpected but promising
119 areas for H₂ exploration. The Paris Basin, with its unique geological features, serves as a focal point for
120 this investigation, potentially positioning it as a H₂-rich geological province. Our research underscores the
121 value of innovative data processing techniques in enhancing the efficiency and scope of geological
122 exploration, particularly in the context of emerging energy resources like natural hydrogen.

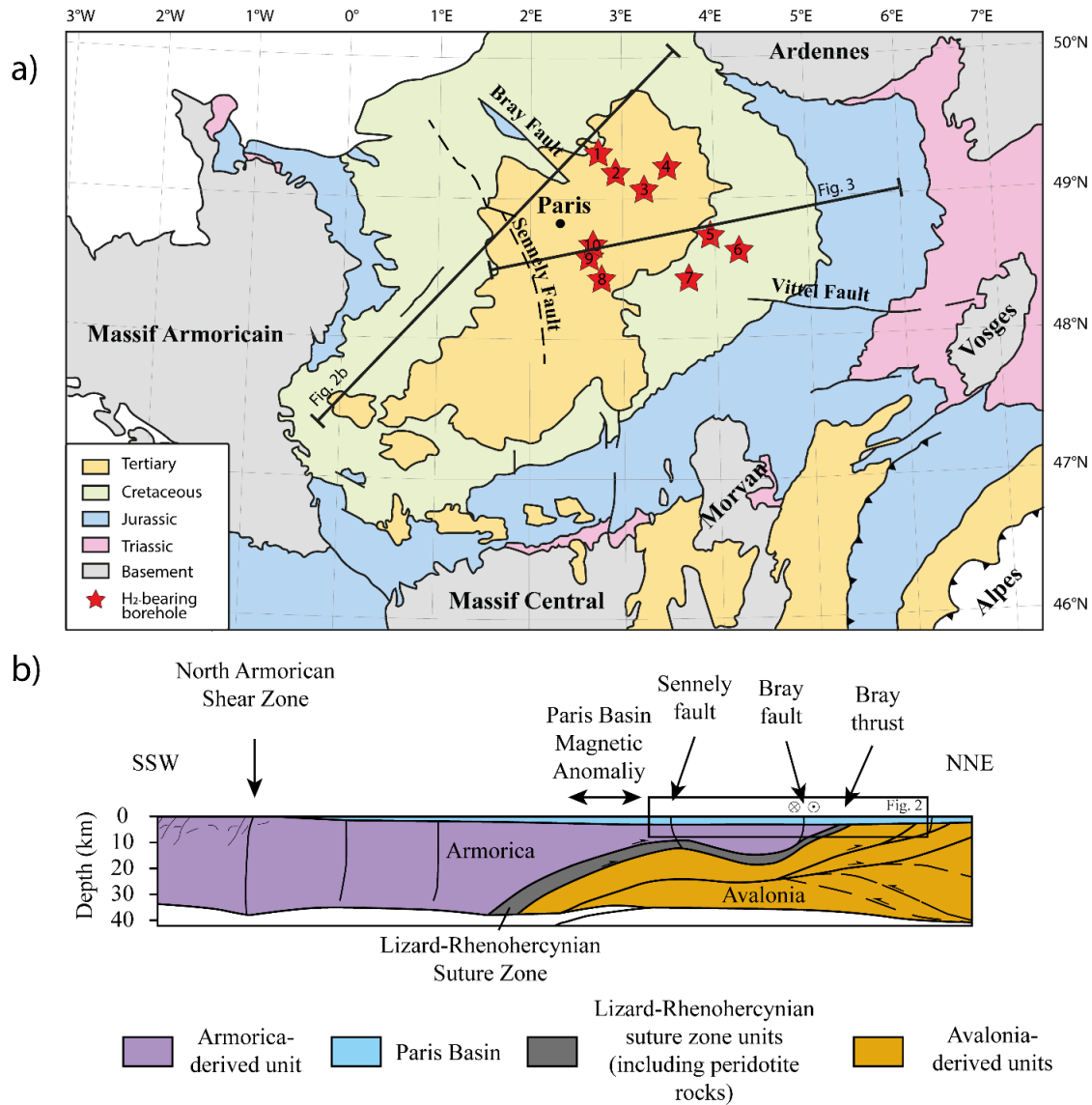
123 **2 Geological context**

124 The Paris Basin, a prominent intracratonic basin, encompasses approximately 3 km of sedimentary
125 deposits spanning from the Trias to present. These deposits overlie the Variscan suture zones, a
126 significant geological feature from the Upper Paleozoic era, as documented in several studies (Fig. 2a;
127 Curnelle and Dubois, 1986; Delmas et al., 2002; Mégnien et al., 1980; Pomerol, 1978). The basin is
128 geographically bounded by four Paleozoic massifs: the Armorican Massif to the south, the Bresse Graben
129 to the southeast, the Vosges Massif to the east, and the Ardennes Massif to the north. The Paris Basin
130 exhibits a distinct geological structure, characterized by concentric outcrops of Meso-Cenozoic rocks.
131 This structure is the result of a series of depositions and erosional processes, as detailed in various studies
132 (Beccaletto et al., 2011; Delmas et al., 2002; Guillocheau et al., 2000). Additionally, the basin extends to
133 connect with the London and Belgium Basins to the northwest and north, respectively (Dercourt et al.,
134 2000).

135 Two major fault systems are prominent in the Paris Basin: the Sennely fault and the Bray fault system
136 (Fig.2). The latter is a N130° dextral strike-slip fault that impacts the sedimentary cover (Matte and Hirn,
137 1988, Raoult and Meilliez, 1987).

138 The basement of the Paris Basin is a lithological and structural inheritance of the Variscan orogeny,
139 which occurred during the Carboniferous period following to the north-south convergence of the
140 Avalonia and Gondwana plates, culminating in the closure of the Rheic Ocean (Averbuch and Piromallo,
141 2012; Ballèvre et al., 2009; Matte, 1986). Seismic tomography beneath the Paris Basin has revealed
142 anomalies in the upper mantle, with V_p velocities oriented along NW-SE axes. These anomalies, situated
143 along the Bray fault, are associated with the Variscan suture zone, indicative of a Variscan paleoslab (Fig.
144 2b; Averbuch and Piromallo, 2012; Cazes et al., 1986). Recent P-wave seismic tomography studies
145 suggest the presence of a subducted paleo-slab beneath a segment of the Bray Fault (Autran et al., 1994;
146 Averbuch and Piromallo, 2012; Matte and Hirn, 1988). Complementary gravimetric and magnetic data
147 along this major fault structure have identified anomalies correlating with granite intrusions (Baptiste,

148 2016; Thébaud et al., 2006). The Lizard-Renohercynian suture zone, as illustrated by the Lizard
 149 ophiolitic complex in southern part of Great Britain, comprises both ultramafic (peridotite, serpentinite)



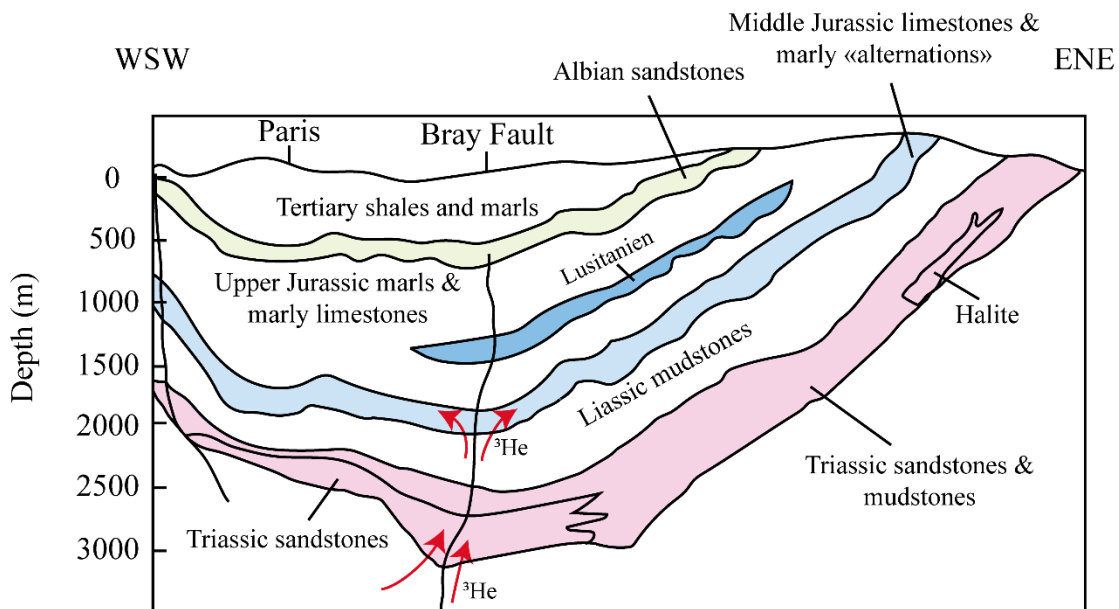
150 and crustal rocks (amphibolite, gneiss, etc.), further elucidated in various studies (Cook et al., 2002, 1998;
 151 Leake and Styles, 1984; Roberts et al., 1993).

152 *Figure 2 : a) The structural map of the Paris Basin displays the main units and the surrounding*
 153 *crystalline massifs (modified from Baptiste, 2016). In this map, the red stars represent the wells showing*
 154 *evidences for the presence of H₂, as identified using the OCR algorithm developed in the study 1 -*
 155 *Longeuil ; 2 - Betz ; 3 - Montreuil Aux Lions ; 4 - Cramaille ; 5 - Connantre 1 and 2 ; 6 - Grandville ; 7 -*
 156 *Saint Martin de Bossenay ; 8 - Hericy ; 9 - Le Luteau ; 10 - Coubert. b) Crustal-scale cross-section*
 157 *through the Variscan orogenic system and the Paris Basin based on the Northern France crustal cross-*
 158 *section (modified from Averbuch and Piromallo, 2012 and Matte and Hirn, 1988).*

159

160 The Parisian Basin, primarily recognized for its hydrocarbon reserves, is characterized by over 3,000
 161 boreholes that have been instrumental in delineating its structural framework. This basin encompasses
 162 several key aquifers and reservoir (Fig. 3). These include: (i) The Triassic Sandstone aquifer, capped by
 163 mudstone and an evaporitic formation, particularly in the central part of the basin with a temperature of
 164 120°C (e.g., Montmirail well; Torelli et al., 2020); (ii) The Middle Jurassic limestone aquifer, containing
 165 geothermal waters with temperatures ranging between 50 to 80°C and (iii) the Lower Cretaceous green
 166 sandstone aquifers. A recent study calculated the geothermal gradient at $T = 10 + 34.9 \cdot z$, (where T is the
 167 temperature in °C and z is the depth in km), derived from an analysis of existing well data and aquifer
 168 temperatures (Bonté et al., 2010; Pinti and Marty, 1998).

169 Furthermore, Pinti and Marty (1998) identified a helium anomaly in the Dogger Formation,
 170 characterized by an unusual excess of mantle-derived ^3He in the Dogger aquifer, particularly near the
 171 Bray fault (Fig. 3). This fault is hypothesized to serve as a conduit for helium-rich fluids, facilitating their
 172 migration through the low-permeability shales that separate the Triassic and Dogger aquifers (Worden
 173 and Matray, 1995).



174

175 *Figure 3 : A schematic cross-section of the Paris Basin, with the main aquifer positions (Modified*
 176 *from Pinti and Marty, (1998)).*

177

178 Integrating geodynamic, geophysical, and geochemical data, it is assumed that a paleo-slab,
 179 composed of mantellic and metamorphic rocks, is connected to the basin via the Bray fault (Bril et al.,

180 1994). The detection of mantle-derived ^3He in the Dogger aquifer suggests a deep structural connection to
181 these formations (Fig. 3).

182 The Paris Basin's geology is particularly promising for H_2 exploration. This potential is attributed to
183 the presence of ultramafic rocks undergoing serpentinization, water radiolysis in granite bodies, the
184 existence of preferential pathways for fluid migration and the excess of ^3He . Additionally, numerous
185 reservoirs within the basin exhibit favorable porosity and permeability characteristics, making them
186 suitable candidates for hydrogen storage. Collectively, these factors underscore the basin's potential as a
187 complete H_2 system from sources to traps.

188

189 **3 Methodology**

190 3.1 Data origin

191 The database used in our research, whose management is delegated to the French Bureau of Hydrocarbon
192 Exploration and Production, encompasses a comprehensive collection of well data. This repository,
193 known as the BEPH database, contains 5,139 records dating back to 1927, covering hydrocarbon
194 exploration activities in both metropolitan France and its overseas territories. However, a significant
195 portion of the database, approximately 36.8 % (equating to 1,893 files), is missing, primarily consisting of
196 End Drilling Reports (EDRs) in PDF format. The database incorporates a diverse array of data, including
197 scanned EDRs, well logs (such as Gamma-ray, etc.), mudlogs, seismic coring, and other relevant
198 documents (site logs, tests, etc.). For the purposes of our study, we concentrated exclusively on the
199 analysis of the EDRs, which comprise 3,246 scanned documents in PDF format, with individual files
200 ranging from 10 to 300 pages.

201 3.2 Pytesseract Screening RFS

202 Given the image-based nature of these documents, conventional keyword search techniques are infeasible,
203 and manual examination would be prohibitively time-consuming. To address this challenge, we employed
204 Optical Character Recognition (OCR) technology. Specifically, we utilized Pytesseract, a Python-based
205 OCR tool that integrates Google's Tesseract-OCR Engine (available at
206 <https://github.com/madmaze/pytesseract>), to convert the EDR PDFs into searchable formats (Fig. S1).

207 The process requires preliminary process of each EDR. As Pytesseract is incapable of directly processing
208 PDF files, we first converted each page of the EDRs into image files (PNG, JPG, etc.) using an initial
209 conversion tool. This tool transforms the scanned PDF images into Python Imaging Library (PIL) format,

210 with each PIL image representing a page from the EDR. Subsequently, Pytesseract OCR processes each
211 page, converting the text into a searchable PDF format, which we labeled as "EDR_reference".
212 To further analyze the newly created searchable database, we employed PyMuPDF, a Python library
213 designed for extracting, analyzing, converting, and manipulating PDF file data. This library facilitates
214 keyword filtering within each searchable PDF, allowing us to extract the file name and the specific page
215 number where the keyword appears, and store this information in a .txt file. This approach significantly
216 streamlines the process of identifying relevant files and their locations, thereby enhancing the efficiency
217 of quality checks and validation. In our case study, we focused on keywords such as "H₂", "Hydrogène".

218 **4 Results**

219 Applying the OCR algorithm to the Paris Basin well database, 141 occurrences were found in the
220 French EDR database containing "Hydrogen" ("hydrogène" in French) and/or "H₂". Initially, each time
221 the word "hydrogen" is detected, *Pytesseract* records it in the results file. However, in the boreholes of
222 the Paris Basin, there are many occurrences of Hydrogen Sulfide (H₂S) which biases the results. The
223 inability to distinguish between "H₂" and "H₂S" can lead to problems, therefore rapid human verification
224 is essential. The main results have been reported in the supplementary materials.

225 After the validation process, only 11 wells of the Paris basin, the presence of the "H₂" or "Hydrogen"
226 keyword is mentioned in their EDR (Tab. S1). In EDR, when hydrogen is detected, geologists propose
227 various hypotheses to explain its presence, such as: i) hydrogen arising from tool deterioration, ii)
228 hydrogen of unknown origin, iii) hydrogen detected but not quantified, iv) trace concentrations of
229 hydrogen in the background gas, and v) hydrogen identified using neutron porosity techniques.

- 230 • The Longueil 1 Well (drilled in 1972), has detected H₂ and N₂ trace (no concentrations
231 reported in the EDR) during the mud gas logging at 3 different depths i) In Lusitanian
232 formation at 988 to 1241m and composed of limestone (porosity of 19.2 %); ii) in the Middle
233 Jurassic at 1241 to 1347m and composed of Massigny Marles (porosity ranging from 9 to
234 19 %) and iii) In Triassic formation at 1916 to 1981 m and composed of Saint Maur Red
235 Clay. The geologist in charge doesn't explain the origin of H₂.
- 236 • The Betz 101 drilling well (drilled in 1963) revealed a concentration of H₂ gas ranging to 3 to
237 6 vol% in Lusitanian formation at a depth of 1325 to 1335 m, however the report does not
238 describe the methodology used for this gas analysis. The Lusitanian formation is mainly
239 composed of limestone with a porosity ranging from 7 to 11 %. The geologist in charge
240 revealed that detecting high H₂ concentrations in the Lusitanian formation in this area is
241 common, but its origin remains unknown.

- 242 • The Montreuil Aux Lions 1 drilling well (drilled in 1988) detected H₂ gas in a bottle sample
243 of 1 liter taken at a depth of 2165-2175 m corresponding to Marles to Calcareous Clay
244 formation in the Dogger. The pressure inside the bottle was 25 bar. The gas measurement
245 revealed a gas composition of H₂ 52 vol%, CH₄ 42 vol%, C₂ 4.3 vol%, C₃ 0.9 vol% and nC₄
246 0.19 vol%. The EDR did not provide any hypothesis about the origin of this H₂
247 concentration.
- 248 • The Cramaille 101 drilling well (drilled in 1961) detected H₂ during the mud gas logging
249 while crossing the Lusitanian formation, which is composed of limestones with a porosity of
250 16.7 % and a permeability ranging from 0.1 to 12 mDy. However, the EDR did not indicate
251 the exact concentration of H₂ gas, and there was no explanation provided for this gas
252 detection.
- 253 • The Connantre 2 drilling well (drilled in 1981), have detected the presence of H₂ and
254 nitrogen from 1508 to 1533 m, the Dogger formation was composed of limestones with
255 porosity ranging from 7 to 11 %. The useful height of the formation was 9.5 m. The
256 methodology for gas analysis is not described in the EDR.
- 257 • The Grandville 109 drilling well (drilled in 1982) has identified during the mud gas logging
258 the presence of H₂ at two different depths i) The Aalenian formation is made up of clayey
259 limestones and ranges from 1159 to 1725 m. The background mud gases have a H₂
260 concentration that ranges from 0.25 to 0.65 vol%. ii) The Triassic formation, spanning from
261 2053 to 2555 m in depth, consists of dolomite, clay, and evaporite. Within the background
262 gases, a concentration of 0.2 vol% of H₂ was detected.
- 263 • The Coubert 1 drilling well (drilled in 1986), has detected H₂ during the mud gas logging in
264 the bottom hole at 2547 m depth but no concentrations are reported in the EDR. The
265 Hercynian formation is mainly composed of Gneiss-type rocks. The gas composition
266 recorded showed unusual fluctuations, with a disappearance of C₄ hydrocarbons and a
267 reduction in C₃ and C₂ concentrations, but an increase in total gas, along with the release of
268 H₂. The main hypothesis proposed by geologists is gas production linked to tool alteration.
- 269 • The Luteau 1 drilling well (drilled in 1986) detected H₂ and CH₄ during the mud gas logging
270 while crossing Keuper from 2569 to 2578 m, which is mainly composed of clay but locally
271 contains anhydrite. Unfortunately, the gas chromatograph (GC) used was unable to

272 distinguish between H₂ and CH₄. The H₂-CH₄ compounds were detected during core
273 sampling in the background gas ranging from 0.6 to 1.1 vol%.

- 274 • The Hericy 1 drilling well (drilled in 1986) detected H₂ and CH₄ in the gas background
275 during the mud gas logging. However, the GC cannot distinguish between them, similar to
276 Luteau 1. This potential H₂ detection occurs during the crossing of Liassic formation
277 composed of calcareous clay. The gas Background is ranging from 1 to 3.5 vol%.
- 278 • The Saint Martin de Bossenay 17 drilling well (drilled in 1976) detected H₂ traces in two
279 different formations. i) The upper Triassic (Rethien) Clayay formation was tested at a depth
280 of 2084 m. They detected H₂ gas but did not report its concentration. The well was open for
281 32 minutes, during which they recovered 20 liters of gas and 0.5 liters of mud. ii) The Upper
282 Triassic formation, made up of sandstones, clay, and anhydrite rocks, was tested at a depth of
283 2295 m. During the test, the well was open for 37 minutes and recovered 410 liters of mud, a
284 small quantity of gas and 120 liters of gasified mud. They also reported that the gas was
285 detected in the same formation as the Saint Martin de Bossenay 201 well. The pressure of
286 196 kg/m² was unstabilized at 2321m.
- 287 • The Jeumont 1 drilling well (drilled in 1963), has detected H₂ in mud gas at two different
288 depths i) At a depth of 4443 m in the Upper Devonian, there is a composition of quartzite and
289 argillite. The detected H₂ is present in background gas at a concentration of 0.5 vol%. ii) At a
290 depth of 4807 m, the Middle Devonian is mainly composed of quartzite and shale. The H₂
291 concentration is also in background gas at a concentration of 1.8 vol%. The H₂ concentration
292 for both depths was unexplained.

293 All the data originate from wells drilled at various times during the 20th century and have not been
294 previously correlated. To comprehend the natural hydrogen potential of this region, it is essential to
295 integrate these data with the knowledge acquired in recent decades and with contemporary geological
296 studies of the Paris Basin. Consequently, a comprehensive compilation of both geochemical and
297 geological knowledge will also be carried out.

298 **5 Discussion**

299 **5.1 Hydrogen Detection and Origin Hypotheses in Various Geological Formations of the** 300 **Paris Basin**

301 According to the OCR algorithm, the drilling wells' location is concentrated within an area of 8600 km² in
302 the middle east of the Paris Basin (Fig. 2a). The H₂ concentration in the Paris Basin is not randomly
303 distributed throughout the formations. It is mainly present in three formations: Lusitanian, Dogger, and
304 Keuper.

305 **5.1.1 The Lusitanian reservoir**

306 Three sites north of the Bray fault—Longueil, Betz, and Cramaille—reported H₂ content while
307 intersecting the Lusitanian formation. According to the Initial interpretations, this would indicate a
308 potential tool degradation. However, H₂ was also detected in the same formation in Longueil and Betz
309 wells. The well geologist revealed in the Betz 101 EDR that detecting H₂ in the Lusitanian formation is
310 common. Therefore, the hypothesis of H₂ production by steel corrosion in Cramaille could be discarded.
311 An alternative hypothesis involves the production of H₂ through mechano-radical reactions occurring
312 during drilling. This suggests that the mechanical crushing of rocks results in the production of fresh Si
313 surfaces that are highly reactive with water, generating H₂ (Hirose et al., 2011; Kita et al., 1982).
314 Nevertheless, the Lusitanian is mainly composed of limestone and contains little to no silica. Lefeuvre
315 (2022) conducted a limestone grinding experiment in a confined atmosphere and demonstrated that this
316 rock did not produce H₂. This leads to questioning the origin of the H₂.

317 **5.1.2 The Dogger reservoir**

318 Investigations into the Dogger formation, specifically at the Montreuil Aux Lions, Connantre, and
319 Grandville wells north of the Bray Fault, have identified H₂ concentrations. At Montreuil Aux Lions, a
320 sampling approach was employed, utilizing a specialized bottle to collect a sample from within the
321 Dogger formation. The analysis of this sample revealed 52 vol% H₂ concentration within a 1-liter vessel
322 under 25 bar pressure. Notably, the hypothesis of H₂ production by mechano-radical processes was
323 discarded due composition of Dogger formation, corresponding to Oolitic limestones. Moreover, this
324 conclusion is reinforced by the fact that the sampling procedure did not take place at the same time as the
325 drilling activities.

326 Gases have been sampled in Dogger formation from geothermal production wellheads during both
327 artesian flow and production under pumping (Fig. 3). These wellheads exhibited pressure ranges from 4
328 to 12 bar, indicative of a monophasic state at depth for such fluids (Marty et al., 1988). Marty et al. (1988)

329 conducted analyses on 34 dissolved gas samples, which were isolated using a vacuum flask vessel half-
330 filled with the separated liquid phase containing the dissolved gases. They recorded H₂ concentrations
331 reaching up to 12 x 10⁻⁵ mol/l (at 71 °C and 9.81 bar). The prevalence of steel corrosion as possible origin
332 for elevated H₂ levels remains a consideration. However, only 9 out of the 34 wells displayed
333 concentrations exceeding 1 mol/l, suggesting a different origin for the elevated H₂ concentrations. These
334 observations support the existence of an H₂-rich aquifer in the Dogger.

335 The Dogger aquifer is also known for the presence of sulfate-reducing, methane-producing bacteria,
336 which are mainly thermophilic (Fouillac et al., 1990). Isolated methane-producing bacteria from
337 Mellaray's well have shown the capability to thrive utilizing H₂ and CO₂ as their sole carbon and energy
338 sources (Daumas et al., 1986; Marty et al., 1993). This observation suggests that the H₂ measured in the
339 Dogger is a source of energy for bacterial communities and it raises questions about the deeper origin of
340 H₂.

341 5.1.3 The Triassic reservoir

342 In the Upper Triassic formation situated south of the Bray Fault, H₂ presence was documented in the
343 drilling wells at Le Luteau and Saint Martin de Bossenay. This formation is characterized by a composite
344 of clay, anhydrite, and sandstones.

345 At Le Luteau, the detected background H₂ concentrations during the drilling might be associated with
346 mechano-radical mechanisms, a hypothesis supported by the silica-rich composition of the rocks.

347 At Saint Martin de Bossenay, H₂ detection occurred during post-drilling production testing, rendering the
348 mechano-radical hypothesis less plausible for this site. It is important to note that no acidification of the
349 well was performed prior to conducting this test. In this formation, the anhydrite may act as a promising
350 sealing rock for trapping H₂.

351 5.1.3 H₂ detection through the basement

352 Lastly, two other wells reached the basement at Coubert and Jeumont, and they revealed the concentration
353 of H₂ at depth. The Coubert well, situated to the south of the Bray fault, traverses a geological formation
354 composed predominantly of Gneiss and quartzite with galena intrusions. At this site, geologists cannot
355 differentiate between methane and H₂ gases due to instrumental reasons. However, a notable diminution
356 in C₄ to C₂ hydrocarbon concentrations suggests a possible H₂ degassing, potentially originating from
357 drilling tools or the surrounding rock matrix as suggested in the EDR. The Jeumont well only revealed H₂
358 concentration during the core sampling of quartzite formation. This observation supports the hypothesis
359 of H₂ generation through mechano-radical processes.

360

361 Due to limited EDR data, deciphering the source of H₂ remains challenging. Geological and geochemical
362 contextualization may offer a starting point for further analysis.

363 5.2 Geological Trends and Structural Analysis of Drilling Wells in the Paris Basin

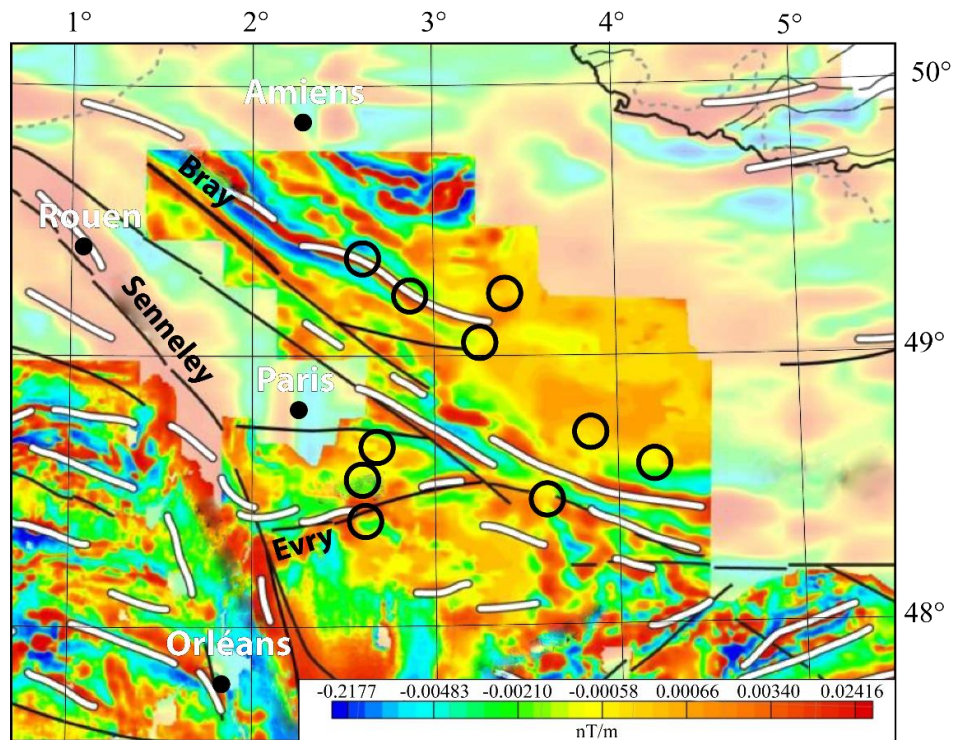
364 Initial observations indicate that the wells Longueil 1, Betz 101, and Montreuil Aux Lions 1, located to
365 the north of the Bray fault delineate a trend of N130° orientation. This aligns with the orientation of the
366 Bray fault, albeit situated approximately 20 km northward. This trend is highlighted and well correlated
367 with the map of the vertical gradient of the pole-reduced magnetic anomaly extended to 600 m (Fig. 4;
368 Baptiste et al., 2016). The vertical gradient technique can be used to identify lithological features,
369 delineate contacts and discern structural variations between distinct geological formations (Baranov,
370 1953). This pattern could correspond the Bray Thrust located by Averbuch and Piromallo (2012) but
371 regarding the seismic cross section this discontinuity doesn't affect the sedimentary cover (Fig. 2b).

372 Contrastingly, the wells Cramaille 101, Connantre 1, 2, and Grandville 109 do not align with this specific
373 trend but are situated within a large regional anomaly. This anomaly has been linked with magmatic
374 rocks, with the axis of this anomaly appears to be correlated with the closure of the Rhenohercynian
375 ocean during the Carboniferous period (Thébault et al., 2006).

376 Regarding the wells located south of the Bray fault (Fig. 4), their distribution is more dispersed and their
377 association with structural features is more complex. These wells are part of the Bloc Evry-Tonnerre, an
378 area where the basement has been mapped through magnetic and gravimetric analysis (Baptiste, 2016).

379 The drilling well Hericy 1 is located on the Evry Fault, while Saint Martin de Bossenay 17 is located on
380 the Lalaye-L Fault (Baptiste, 2016). The map reveals the presence of basic rocks along the Evry fault, and
381 a combination of gneissic or granitic rocks interspersed with Néoproterozoic/Paleozoic formations along
382 the Lalaye-L Fault. The two other wells, Le Luteau 1 and Coubert 1, while not associated with any
383 specific faults, are located above granodiorite bedrock.

384 While the majority of the wells' locations appear to be correlated with fault lines, further investigation is
 385 needed to determine if these faults could act as conduits for fluid migration.



386 *Figure 4 : Map of the vertical gradient of the magnetic anomaly reduced to the pole and extended to*
 387 *600 meters. The black circle corresponds to the H₂-bearing well (Modified from Baptiste, 2016).*

388 5.3 Characteristics and Deep Fluid Helium Studies of the Dogger Aquifer in the Paris 389 Basin

390 The Paris Basin is characterized by several key aquifers, including Triassic sandstones, Dogger
 391 limestones, Lusitanian limestones, and Albian sandstones (Fig. 3). Among these, the Dogger aquifer has
 392 been the primary focus of numerous studies, primarily due to its notable helium concentration (Bril et al.,
 393 1994; Castro et al., 1998a, 1998b; Marty et al., 1993, 1988; Pinti and Marty, 1998)

394 The Dogger aquifer exhibits a relatively consistent helium concentration and isotope ratio, though it
 395 presents minor variations in water chemistry (Marty et al., 1993). According to studies by Marty et al.
 396 (1988), the reported free gas concentration of helium in the aquifer ranging from 1.02 to 4.65×10^{-5} mol/l
 397 (at 70 ± 10 °C, the pressure is not reported). Additionally, isotopic analyses have revealed a distinct
 398 excess of ³He, indicative of a mantle-derived origin. Pinti and Marty, (1993) suggest that the enrichment
 399 in mantle-derived ³He, alongside high ⁴He concentrations, may be attributed to the influx of basement
 400 fluids into the Dogger and potentially to in-situ production within the Middle Jurassic formation.

401 To explain the high helium concentration in the aquifer, one plausible explanation is the presence of a
402 preferential migration pathway, notably the Bray-Vittel Fault (Fig. 3). This fault affects both the
403 sedimentary cover and the basement, and can serve as intermittent vertical drains for helium-rich fluids
404 across the 700m of low-permeability rocks that separate these aquifers (Bril et al., 1994; Pinti and Marty,
405 1998; Worden and Matray, 1995).

406 The analysis of the Dogger aquifer has revealed fluid migration along the major faults, while our OCR
407 analysis has pinpointed wells exhibiting H₂ anomalies correlated with these faults. These findings suggest
408 the existence of a potentially fertile H₂ system.

409 5.4 A putative H₂ system ?

410 The potential for H₂ exploration in the Paris Basin is closely linked to its geodynamic characteristics and
411 structural features, particularly those associated with the closure of the Lizard-Rhenohercynian ocean.
412 This suture zone is composed of ultramafic rocks, including peridotites and amphibolites, which are able
413 to produce H₂ through hydrothermal reactions such as serpentinization. The current temperature near the
414 basin/basin discontinuity is approximately 120°C (Pinti and Marty, 1998), significantly lower than the
415 250 to 300°C typically required for optimal H₂ production kinetics (Malvoisin et al., 2012; McCollom et
416 al., 2016). However, a significant aspect of the Lizard complex is its composition, consisting of dunite,
417 which is largely serpentinized and contains magnetite (Leake and Styles, 1984). Recent findings by
418 Geymont et al. (2023) have revealed the potential of magnetite to facilitate H₂ production at relatively
419 lower temperatures through hydrothermal alteration processes. Therefore, in this geological context,
420 serpentinized dunite, particularly rich in magnetite, may represent a viable source rock for H₂ generation.
421 This raises the question of the actual production of H₂.

422 To the north of this closure zone, magnetic and gravimetric anomalies suggest the presence of granitic
423 formations, which can facilitate H₂ generation via radiolysis of water, a process independent of rock
424 temperature (Lin et al., 2005b; Sherwood Lollar et al., 2006).

425 A key factor in these H₂-producing processes is the presence of a water source, originating from a
426 recharge zone. The basin's sedimentary cover and basement are influenced by regional tectonic
427 lineaments, notably the Bray-Vittel and Rouen-Couy faults, which may act as conduits for vertical fluid
428 migration. Studies on noble gases suggest a vertical flow of fluids through the Rouen-Couy fault,
429 allowing water infiltration into the sedimentary layer through this discontinuity, eventually reaching the
430 basement (Pinti and Marty, 1998; Rouchet, 1981). Additionally, the Paris Basin hosts multiple aquifers,
431 potentially serving as sources for water essential to these reactions.

432 Helium analysis within the basin has provided insights into fluid migration patterns, with mantle-derived
433 helium detected in the Dogger aquifer, as evidenced by the excess of ³He. The H₂ produced in the

434 basement may migrate through the Bray-Vittel fault and major detachments, and reach the aquifer. The
435 Triassic and Jurassic formation, are marked by evaporitic rocks and clayey rock, offering effective sealing
436 properties for H₂ entrapment. Furthermore, the temperature in the Triassic formation seems suitable for
437 H₂ trapping over geological time, being too hot for microbial activity and too cold for efficient abiotic
438 reactions involving H₂ (Lefeuvre et al., 2022).

439 The Paris Basin stand for a good case study for natural H₂ exploration. All the essential components
440 necessary for the establishment of a H₂ system are gathered: i) a water source facilitating H₂ production,
441 ii) iron-rich and granitic rocks, iii) preferential migration pathways along faults impacting both the
442 basement and sedimentary layers, and iv) efficient reservoirs characterized by the presence of clay,
443 evaporites, and aquifers, which may act as effective seals.

444 **5 Conclusions**

445 After processing the BEPH database with an OCR algorithm, we discovered multiple wells that detected
446 H₂ gas. First, across France, several drilling wells have been identified where H₂ concentrations are
447 documented in their EDR. The distribution of these wells is not random in terms of the geological
448 context, they are frequently situated near mantle bodies at shallow depths. This discovery should lead to
449 further research.

450 In the Paris Basin case, the OCR algorithm revealed four main formations in which H₂ has been detected:
451 Lusitanien formation, Dogger aquifer, Triassic aquifer and in basement. A maximum of 52 vol% of H₂
452 was obtained in the dogger, whereas up to 6 vol% has been measured in the lusitanian. In the others
453 formations, the concentration of H₂ is not measured, but its presence is still reported. These wells are
454 situated in a small area in the central-east of the Paris Basin, and their distribution does not seem random.
455 All of them are situated along the Bray fault and the Bray thrust, which are N°130 faults that affect both
456 the basement and the sedimentary cover. The basement comprises rocks that have the potential to be
457 sources of H₂, such as peridotite or granitic rocks. An excess of ³He is reported in the Dogger Formation,
458 suggesting a contribution from the mantle and deep fluid migration. Finally, the evaporite and clay
459 formation reported in the basin represent a promising trap for H₂.

460 **Acknowledgments**

461 This work was conducted in collaboration of CVA Group. Nicolas Lefeuvre acknowledges CVA
462 Group for the access to their database. Vincent Roche, Guilhem Scheiblin are warmly thanked for his
463 support in understanding the geology of the Paris basin.

464 **References**

- 465 Averbuch, O., & Piromallo, C. (2012). Is there a remnant Variscan subducted slab in the mantle beneath
466 the Paris basin? Implications for the late Variscan lithospheric delamination process and the Paris basin
467 formation. *Tectonophysics*, 558–559, 70–83. <https://doi.org/10.1016/j.tecto.2012.06.032>
- 468 Baptiste, J., Martelet, G., Faure, M., Beccaletto, L., Reninger, P.-A., Perrin, J., & Chen, Y. (2016).
469 Mapping of a buried basement combining aeromagnetic, gravity and petrophysical data: The substratum
470 of southwest Paris Basin, France. *Tectonophysics*, 683, 333–348.
471 <https://doi.org/10.1016/j.tecto.2016.05.049>
- 472 Baranov, V. (1953). Calcul du gradient vertical du champ de gravité ou du champ magnétique mesuré à la
473 surface du sol. *Geophysical Prospecting*, 1(3), 171–191. [https://doi.org/10.1111/j.1365-](https://doi.org/10.1111/j.1365-2478.1953.tb01139.x)
474 [2478.1953.tb01139.x](https://doi.org/10.1111/j.1365-2478.1953.tb01139.x)
- 475 Bonté, D., Guillou-Frottier, L., Garibaldi, C., Bourguin, B., Lopez, S., Bouchot, V., & Lucazeau, F.
476 (2010). Subsurface temperature maps in French sedimentary basins: new data compilation and
477 interpolation. *Bulletin de La Société Géologique de France*, 181(4), 377–390.
478 <https://doi.org/10.2113/gssgfbull.181.4.377>
- 479 Boreham, C. J., Sohn, J. H., Cox, N., Williams, J., Hong, Z., & Kendrick, M. A. (2021). Hydrogen and
480 hydrocarbons associated with the Neoproterozoic Frog's Leg Gold Camp, Yilgarn Craton, Western Australia.
481 *Chemical Geology*, 575, 120098. <https://doi.org/10.1016/j.chemgeo.2021.120098>
- 482 Bril, H., Velde, B., Meunier, A., & Iqdari, A. (1994). Effects of the “pays de Bray” fault on fluid
483 paleocirculations in the Paris basin dogger reservoir, France. *Geothermics*, 23(3), 305–315.
484 [https://doi.org/10.1016/0375-6505\(94\)90006-X](https://doi.org/10.1016/0375-6505(94)90006-X)
- 485 Castro, M. C., Jambon, A., De Marsily, G., & Schlosser, P. (1998). Noble gases as natural tracers of water
486 circulation in the Paris Basin: 1. Measurements and discussion of their origin and mechanisms of vertical
487 transport in the basin. *Water Resources Research*, 34(10), 2443–2466.
488 <https://doi.org/10.1029/98WR01956>
- 489 Castro, M. C., Goblet, P., Ledoux, E., Violette, S., & De Marsily, G. (1998). Noble gases as natural
490 tracers of water circulation in the Paris Basin: 2. Calibration of a groundwater flow model using noble gas
491 isotope data. *Water Resources Research*, 34(10), 2467–2483. <https://doi.org/10.1029/98WR01957>
- 492 Chevrot, S., Sylvander, M., Diaz, J., Martin, R., Mouthereau, F., Manatschal, G., et al. (2018). The non-
493 cylindrical crustal architecture of the Pyrenees. *Scientific Reports*, 8(1), 9591.
494 <https://doi.org/10.1038/s41598-018-27889-x>
- 495 Chevrot, S., Sylvander, M., Villaseñor, A., Díaz, J., Stehly, L., Boué, P., et al. (2022). Passive imaging of
496 collisional orogens: a review of a decade of geophysical studies in the Pyrénées. *BSGF - Earth Sciences*
497 *Bulletin*, 193, 1. <https://doi.org/10.1051/bsgf/2021049>

- 498 Daumas, S., Lombart, R., & Bianchi, A. (1986). A bacteriological study of geothermal spring waters
499 dating from the dogger and trias period in the Paris Basin. *Geomicrobiology Journal*, 4(4), 423–433.
500 <https://doi.org/10.1080/01490458609385947>
- 501 Donzé, F.-V., Truche, L., Shekari Namin, P., Lefeuvre, N., & Bazarkina, E. F. (2020). Migration of
502 Natural Hydrogen from Deep-Seated Sources in the São Francisco Basin, Brazil. *Geosciences*, 10(9), 346.
503 <https://doi.org/10.3390/geosciences10090346>
- 504 Etiopé, G., Judas, J., & Whitar, M. J. (2015). Occurrence of abiogenic methane in the eastern United Arab
505 Emirates ophiolite aquifer. *Arabian Journal of Geosciences*, 8(12), 11345–11348.
506 <https://doi.org/10.1007/s12517-015-1975-4>
- 507 Fiebig, J., Woodland, A. B., Spangenberg, J., & Oschmann, W. (2007). Natural evidence for rapid
508 abiogenic hydrothermal generation of CH₄. *Geochimica et Cosmochimica Acta*, 71(12), 3028–3039.
509 <https://doi.org/10.1016/j.gca.2007.04.010>
- 510 Fouillac, C., Fouillac, A., & Criaud, A. (1990). Sulphur and oxygen isotopes of dissolved sulphur species
511 in formation waters from the Dogger geothermal aquifer, Paris Basin, France. *Applied Geochemistry*,
512 5(4), 415–427. [https://doi.org/10.1016/0883-2927\(90\)90018-Z](https://doi.org/10.1016/0883-2927(90)90018-Z)
- 513 Hirose, T., Kawagucci, S., & Suzuki, K. (2011). Mechanoradical H₂ generation during simulated faulting:
514 Implications for an earthquake-driven subsurface biosphere: H₂ generation during earthquakes.
515 *Geophysical Research Letters*, 38(17). <https://doi.org/10.1029/2011GL048850>
- 516 Jammes, S., Lavier, L., & Manatschal, G. (2010). Extreme crustal thinning in the Bay of Biscay and the
517 Western Pyrenees: From observations to modeling: modelization of extreme crustal thinning.
518 *Geochemistry, Geophysics, Geosystems*, 11(10), n/a-n/a. <https://doi.org/10.1029/2010GC003218>
- 519 Johnson, J. E., Mienert, J., Plaza-Faverola, A., Vadakkepuliambatta, S., Knies, J., Bünz, S., et al. (2015).
520 Abiogenic methane from ultraslow-spreading ridges can charge Arctic gas hydrates. *Geology*, 43(5), 371–
521 374. <https://doi.org/10.1130/G36440.1>
- 522 Kita, I., Matsuo, S., & Wakita, H. (1982). H₂ generation by reaction between H₂O and crushed rock: An
523 experimental study on H₂ degassing from the active fault zone. *Journal of Geophysical Research: Solid*
524 *Earth*, 87(B13), 10789–10795. <https://doi.org/10.1029/JB087iB13p10789>
- 525 Lefeuvre, N., Truche, L., Donzé, F.-V., Gal, F., Tremosa, J., Fakoury, R.-A., et al. (2022). Natural
526 hydrogen migration along thrust faults in foothill basins: The North Pyrenean Frontal Thrust case study.
527 *Applied Geochemistry*, 145, 105396. <https://doi.org/10.1016/j.apgeochem.2022.105396>
- 528 Lefeuvre, Nicolas, Truche, L., Donzé, F., Ducoux, M., Barré, G., Fakoury, R., et al. (2021). Native H₂
529 Exploration in the Western Pyrenean Foothills. *Geochemistry, Geophysics, Geosystems*, 22(8),
530 e2021GC009917. <https://doi.org/10.1029/2021GC009917>

- 531 Lehuteur, M., Chevrot, S., Villaseñor, A., Masini, E., Saspiturry, N., Lescoutre, R., et al. (2021). Three-
532 dimensional shear velocity structure of the Mauléon and Arzacq Basins (Western Pyrenees). *BSGF -*
533 *Earth Sciences Bulletin*, 192, 47. <https://doi.org/10.1051/bsgf/2021039>
- 534 Lin, L.-H., Slater, G. F., Sherwood Lollar, B., Lacrampe-Couloume, G., & Onstott, T. C. (2005). The
535 yield and isotopic composition of radiolytic H₂, a potential energy source for the deep subsurface
536 biosphere. *Geochimica et Cosmochimica Acta*, 69(4), 893–903. <https://doi.org/10.1016/j.gca.2004.07.032>
- 537 Maiga, O., Deville, E., Laval, J., Prinzhofer, A., & Diallo, A. B. (2023). Characterization of the
538 spontaneously recharging natural hydrogen reservoirs of Bourakebougou in Mali. *Scientific Reports*,
539 13(1), 11876. <https://doi.org/10.1038/s41598-023-38977-y>
- 540 Malvoisin, B., Brunet, F., Carlut, J., Rouméjon, S., & Cannat, M. (2012). Serpentinization of oceanic
541 peridotites: 2. Kinetics and processes of San Carlos olivine hydrothermal alteration. *Journal of*
542 *Geophysical Research: Solid Earth*, 117(B4). <https://doi.org/10.1029/2011JB008842>
- 543 Marcaillou, C., Muñoz, M., Vidal, O., Parra, T., & Harfouche, M. (2011). Mineralogical evidence for H₂
544 degassing during serpentinization at 300°C/300bar. *Earth and Planetary Science Letters*, 303(3–4), 281–
545 290. <https://doi.org/10.1016/j.epsl.2011.01.006>
- 546 Marty, B., Criaud, A., & Fouillac, C. (1988). Low enthalpy geothermal fluids from the Paris sedimentary
547 basin—1. Characteristics and origin of gases. *Geothermics*, 17(4), 619–633. <https://doi.org/10.1016/0375->
548 6505(88)90047-8
- 549 Marty, Bernard, Torgersen, T., Meynier, V., O’Nions, R. K., & De Marsily, G. (1993). Helium isotope
550 fluxes and groundwater ages in the Dogger Aquifer, Paris Basin. *Water Resources Research*, 29(4), 1025–
551 1035. <https://doi.org/10.1029/93WR00007>
- 552 Matte, P., & Hirn, A. (1988). Seismic signature and tectonic cross section of the Variscan Crust in
553 western France. *Tectonics*, 7(2), 141–155. <https://doi.org/10.1029/TC007i002p00141>
- 554 Mayhew, L. E., Ellison, E. T., McCollom, T. M., Trainor, T. P., & Templeton, A. S. (2013). Hydrogen
555 generation from low-temperature water–rock reactions. *Nature Geoscience*, 6(6), 478–484.
556 <https://doi.org/10.1038/ngeo1825>
- 557 McCollom, T. M., & Donaldson, C. (2016). Generation of Hydrogen and Methane during Experimental
558 Low-Temperature Reaction of Ultramafic Rocks with Water. *Astrobiology*, 16(6), 389–406.
559 <https://doi.org/10.1089/ast.2015.1382>
- 560 Mitrofan, H., Marin, C., Chitea, F., Cadicheanu, N., Povară, I., Tudorache, A., et al. (2021). Multi-
561 kilometre long pathway of geofluids migration: Clues concerning an ophiolite serpentinization setting
562 possibly responsible for the inferred abiotic provenance of methane in thermal water outflows of the
563 South-West Carpathians (Romania). *Terra Nova*, 33(1), 56–73. <https://doi.org/10.1111/ter.12491>

- 564 Moretti, I., Prinzhofer, A., Françolin, J., Pacheco, C., Rosanne, M., Rupin, F., & Mertens, J. (2021).
565 Long-term monitoring of natural hydrogen superficial emissions in a brazilian cratonic environment.
566 Sporadic large pulses versus daily periodic emissions. *International Journal of Hydrogen Energy*, *46*(5),
567 3615–3628. <https://doi.org/10.1016/j.ijhydene.2020.11.026>
- 568 Newcombe, R. B. (1935). Natural gas fields of Michigan.
- 569 Pinti, D. L., & Marty, B. (1998). The origin of helium in deep sedimentary aquifers and the problem of
570 dating very old groundwaters. *Geological Society, London, Special Publications*, *144*(1), 53–68.
571 <https://doi.org/10.1144/GSL.SP.1998.144.01.05>
- 572 Prinzhofer, A., Tahara Cissé, C. S., & Diallo, A. B. (2018). Discovery of a large accumulation of natural
573 hydrogen in Bourakebougou (Mali). *International Journal of Hydrogen Energy*, *43*(42), 19315–19326.
574 <https://doi.org/10.1016/j.ijhydene.2018.08.193>
- 575 Rouchet, J. du. (1981). Stress fields, a key to oil migration. *AAPG Bulletin*, *65*(1), 74–85.
576 <https://doi.org/10.1306/2F919774-16CE-11D7-8645000102C1865D>
- 577 Sauvage, J. F., Flinders, A., Spivack, A. J., Pockalny, R., Dunlea, A. G., Anderson, C. H., et al. (2021).
578 The contribution of water radiolysis to marine sedimentary life. *Nature Communications*, *12*(1), 1297.
579 <https://doi.org/10.1038/s41467-021-21218-z>
- 580 Sherwood, B., Fritz, P., Frape, S., Macko, S., Weise, S., & Welhan, J. (1988). Methane occurrences in the
581 Canadian Shield. *Chemical Geology*, *71*(1–3), 223–236. [https://doi.org/10.1016/0009-2541\(88\)90117-9](https://doi.org/10.1016/0009-2541(88)90117-9)
- 582 Sherwood Lollar, B., Lacrampe-Couloume, G., Slater, G. F., Ward, J., Moser, D. P., Gihring, T. M., et al.
583 (2006). Unravelling abiogenic and biogenic sources of methane in the Earth's deep subsurface. *Chemical*
584 *Geology*, *226*(3–4), 328–339. <https://doi.org/10.1016/j.chemgeo.2005.09.027>
- 585 Smith, N. J. P., Shepherd, T. J., Styles, M. T., & Williams, G. M. (2005). Hydrogen exploration: a review
586 of global hydrogen accumulations and implications for prospective areas in NW Europe. *Geological*
587 *Society, London, Petroleum Geology Conference Series*, *6*(1), 349–358. <https://doi.org/10.1144/0060349>
- 588 Smith, R. (2007). An Overview of the Tesseract OCR Engine. In *Ninth International Conference on*
589 *Document Analysis and Recognition (ICDAR 2007) Vol 2* (pp. 629–633). Curitiba, Parana, Brazil: IEEE.
590 <https://doi.org/10.1109/ICDAR.2007.4376991>
- 591 Thébault, E., Manda, M., & Schott, J. J. (2006). Modeling the lithospheric magnetic field over France by
592 means of revised spherical cap harmonic analysis (R-SCHA). *Journal of Geophysical Research: Solid*
593 *Earth*, *111*(B5), 2005JB004110. <https://doi.org/10.1029/2005JB004110>
- 594 Torelli, M., Traby, R., Teles, V., & Ducros, M. (2020). Thermal evolution of the intracratonic Paris
595 Basin: Insights from 3D basin modelling. *Marine and Petroleum Geology*, *119*, 104487.
596 <https://doi.org/10.1016/j.marpetgeo.2020.104487>

- 597 Truche, L., Joubert, G., Dargent, M., Martz, P., Cathelineau, M., Rigaudier, T., & Quirt, D. (2018). Clay
598 minerals trap hydrogen in the Earth's crust: Evidence from the Cigar Lake uranium deposit, Athabasca.
599 *Earth and Planetary Science Letters*, *493*, 186–197. <https://doi.org/10.1016/j.epsl.2018.04.038>
- 600 Tugend, J., Manatschal, G., Kusznir, N. J., Masini, E., Mohn, G., & Thinon, I. (2014). Formation and
601 deformation of hyperextended rift systems: Insights from rift domain mapping in the Bay of Biscay-
602 Pyrenees. *Tectonics*, *33*(7), 1239–1276. <https://doi.org/10.1002/2014TC003529>
- 603 Warr, O., Giunta, T., Ballentine, C. J., & Sherwood Lollar, B. (2019). Mechanisms and rates of 4He ,
604 40Ar , and H_2 production and accumulation in fracture fluids in Precambrian Shield environments.
605 *Chemical Geology*, *530*, 119322. <https://doi.org/10.1016/j.chemgeo.2019.119322>
- 606 Worden, R., & Matray, J. (1995). Cross formational flow in the Paris Basin. *Basin Research*, *7*(1), 53–66.
607 <https://doi.org/10.1111/j.1365-2117.1995.tb00095.x>